Signal Deformation Monitoring for Anomalous Multipath Threats

R. Eric Phelts and Todd Walter, *Stanford University*

ABSTRACT

The current WAAS signal quality monitor algorithm was designed to mitigate anomalous signal distortions. This paper assesses the ability of this monitor mitigate distortions produced from satellite-induced multipath. Leveraging experience from the SVN-49 anomaly, a single-reflection signal threat model is defined and expanded to include an elevation-angle dependence, which may potentially reduce observability of distortions viewed from widely-distributed monitor receivers. Next, the range errors for both single-frequency and dual-frequency aviation users are modeled relative to the monitor's ability to detect them. It is shown that the existing WAAS signal deformation monitor can protect both single and dual-frequency aviation users against a wide range of SV-induced, single-reflection multipath parameters despite significant attenuation of monitor sensitivity due to elevation-angle dependence.

BACKGROUND

The threat of anomalous signal deformations has existed for users of high-integrity differential GNSS navigation systems for many years. Developers of SBAS and GBAS, in particular, originally analyzed that event and proposed several types of anomalous distortions that, without monitoring and detection, could pose a hazard to aviation users. Subsequently, a threat model that encompassed that thinking was proposed and later adopted as the standard by ICAO in 2000 [1]. That threat model specifically identified two classes of anomalous deformations—digital and analog—to capture the general characteristics of distortions observed on the SV-19 fault. Further, the model was ultimately expanded and proposed as representative worst case for all anomalous signal deformation faults. Signal deformation monitors were subsequently developed to mitigate any/all SV-induced distortions using that ICAO threat model for validation.

SVN-49 anomaly in 2009 was caused by an internal reflection in the signal payload; it resembled multipath. That anomaly is not considered a fault, however, because the satellite was never declared healthy. No WAAS users were ever at risk of exposure. Still, the validation threat model was proposed to account for general signal distortions and anomalous multipath is a specific type of distortion against which validated monitors may be assessed. The SVN-49 anomaly was also peculiar in that it had an elevation angle-dependence. (See Figure 1.) That potentially challenges detection capabilities for networks that observe the satellite from widely-separated locations.

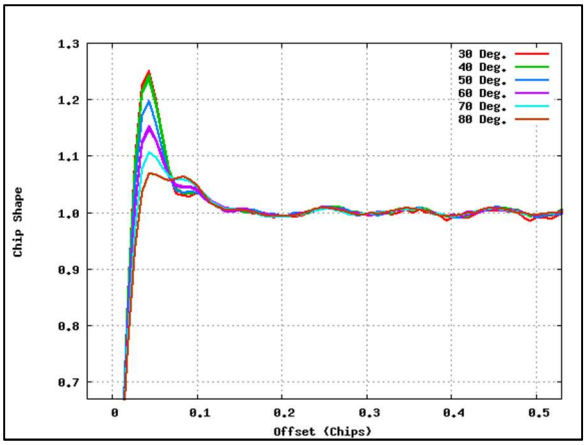

Figure 1. L1 C/A chip shape measured for specific elevation angles for SVN-49 (PRN-01) as measured by an 18 MHz NovAtel receiver. [2]

Previous work has broadly assessed the capability of the WAAS signal quality monitor to protect single-frequency aviation users against the multipath threat [3]. However, relatively little has been done to address

users of dual-frequency WAAS where range errors due to biases are larger while error bounds are reduced. In addition, to date, nothing has been done to account for the potential elevation-angle variations exhibited by anomalous multipath of the type observed on SVN-49. That effect is potentially significant for WAAS monitoring, which relies on a wide network of reference stations distributed across North America. WAAS also traditionally presumes the observation is independent of elevation angle. This paper seeks to assess the existing WAAS signal deformation monitor capability to mitigate the elevation angle-dependent multipath threat for both single and dual-frequency WAAS users.

ANALYSIS

Single-Reflection Threat Model

A simple signal-reflection model (with a reflected signal scale parameter *R* and delay offset, *d*) first was introduced in [3] as a model of this fault model against which to evaluate the WAAS signal deformation monitor. The equation for this threat model—a (single) reflection corrupted C/A code $c(t)$—is given below.

$$\begin{aligned} c(t) &= c_{ideal}(t) + R \cdot c_{ideal}(t) \\ &= c_{ideal}(t) + R \cdot c_{ideal}(t-d) \end{aligned} \quad (1)$$

Traditionally, signal deformation monitor analyses presume the transmitted code $c(t)$ affects the ground receivers and the user receivers equivalently. However, multipath threats may cause different receivers to experience different range errors as a function of the elevation angle of their lines of sight to the satellite. This has the potential to "blind" the monitor to the distortion while a user experiences its full effects. Accordingly, this effect is modeled as a reduction in the monitor measurements relative to those of the user. This effectively adds a third parameter to the two-parameter model above.

Table 1. Parameter limits for the Single-Reflection (Multipath) Threat Model

Parameter	Range
A	-0.99 to 0.99
d (m)	0 to 100 m
β	-10 dB to 0 dB (0.1 to 1)

The parameter ranges of the reflected code $c_{MP}(t) = R \cdot c_{ideal}(t-d)$ and the monitor attenuation factor (β) are provided in Table 1.

User Receiver Configurations

The Minimum Operational Performance Standard (MOPS) version DO-229D describes the allowed receiver configuration for L1-only aviation users of WAAS [4]. These include constraints on discriminator type, correlator spacing, bandwidth, and pre-correlation filter differential group-delay.

Similar constraints for dual-frequency users are not yet finalized but have been proposed. The design space for these receivers will be far more limited in order to reduce the magnitude of the potential errors due to signal deformation threats of all kinds. The discriminator spacing and bandwidth constraints for the single-frequency and dual-frequency receivers modeled in this paper are illustrated in Figures 1 through 3. (For this paper, ΔΔ receivers were not modeled for single-frequency users.) More details on these configurations are provided in Table 2.

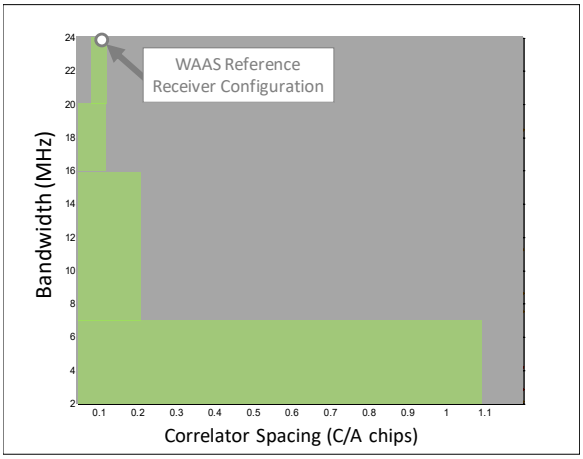

Figure 1. Current WAAS user receiver configurations for single-frequency (L1 C/A-code) EML users.

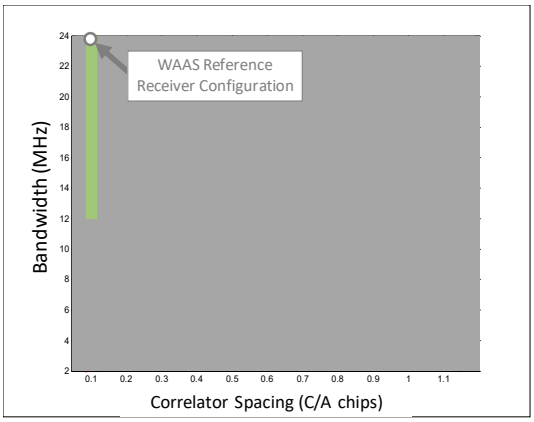

Figure 2. WAAS user receiver configurations for Dual-frequency Users (L1 C/A-code)

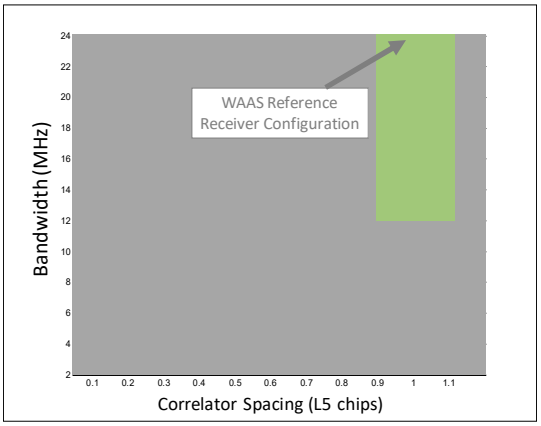

Figure 3. WAAS user receiver configurations for Dual-frequency Users (L5)

Signal Deformation Monitor

The current WAAS signal deformation monitor (and reference receiver) is a network of 138 NovAtel G-III receivers distributed throughout North America. The receivers have 24 MHz front end bandwidth and each uses an early-minus-late (EML) discriminator with 0.1-chip spacing. This receiver forms the differential correction applied to WAAS users.

In addition, the G-III provides 9 correlator outputs on each channel that are used to measure the symmetry of the correlation peak. A WAAS detection metric is simply a linear combination of those correlator outputs according to

$$d^i = \frac{1}{P}\sum_{x=1}^{8} \alpha_x r_x^i \ . \qquad (2)$$

Table 2. User Receiver Constraints Assumed for the SDM Modeling Analysis

Signal Tracking Capability	L1-Only	Dual-Frequency
Discriminator Type	Early-minus-Late (EML) and Double-delta (ΔΔ)	L1: Early-minus-Late (EML) L5: Early-minus-Late (EML)
Correlator Spacing	EML: 0.045-1.2 chips (max) ΔΔ: (Not modeled here) (Varies with bandwidth constraint as described in [4])	L1: 0.08-0.12 chips L5: 0.9-1.1 chips
Bandwidth (MHz)	EML: 2-24MHz ΔΔ: (Not modeled here) (Varies with correlator spacing constraint as described in [4])	L1: Same as L1-only L5: 12-24MHz
Group Delay (ns)	0-600ns (Varies with bandwidth constraint as described in [4])	L1: 0-600ns (Varies with bandwidth constraint [6]) L5: 0-150ns

In the above equation, P is the prompt correlator (at an offset of 0 chips) and α_x is a constant. Finally, a single detection metric is referenced to the nominal, undistorted signal according to

$$D^i = \frac{\left| d^i - \underset{i}{\text{median}}(d^i) \right|}{\text{Threshold}} \qquad (3)$$

In the above equation, the threshold is $K^*\sigma_{mon}$ (where K is a constant set by the false-alarm probability), and σ_{mon} is the nominal monitor noise. The undistorted metric is represented by the median of that metric across all SVs in view. In modeling analyses, however, the nominal is simply the filtered, undistorted signal.

In practice, the current WAAS SDM algorithm takes the maximum over 4 such metrics to form a single threshold-normalized detection test which determines the ultimate detection performance for the monitor. The details on these metrics is provide in [5].

For subsequent sensitivity analyses used in this paper, Equation (3) is scaled by the monitor attenuation factor β, where 0.1 to 1.0 (-10 dB $\leq \beta \leq$ 0 dB).

$$D^i = \frac{\left| d^i \text{-median}_i(d^i) \right|}{\text{Threshold}} \beta \quad (4)$$

It is further assumed the fault exists on an SV that is well-observed by the monitor and is in steady-state. (Transient and spontaneous-onset fault analyses are not included here.) Accordingly, the monitor threshold and the range error limits for the satellite are at a minimum. Attenuation of the monitor metric is expected to account for the potentially significant difference in elevation angles of many the WAAS reference stations' lines of sight relative to the SV.

Anomalous SV Multipath Assumptions

The SVN-49 anomaly was found to be well-modeled by a single-reflection at a relative delay of approximately 11 meters, and the maximum relative amplitude of the SVN-49 anomaly was less than 10% of the direct ray. [2] Due to physical SV dimensions, it is assumed that relative delays of SV multipath should be no more than approximately twice what was observed there. In this paper, a 20 meters limit is proposed as a reasonable limit. But, for completeness, reflections at more extreme delays ($\leq$ 100 meters) are also analyzed. It is difficult to intuit physical constraints on the strength of the reflection relative amplitude. This analysis, however, assumes the maximum reflection amplitude can be as large as that of the direct ray.

Fault Mode and Error Assumptions

As with the standard ICAO signal deformation threat model for signal deformations, there are three separate fault cases which must be mitigated with the single-reflection threat for dual-frequency WAAS users. These are as follows:

1) A fault occurs on L1 only
2) A fault occurs on L5 only
3) A fault occurs on L1 and L5 simultaneously

In each of the above cases, the maximum user errors associated with the fault are scaled according to the dual-frequency combination factors associated with each signal—2.26 and 1.26 applied to L1 and L5 errors, respectively.

Single-frequency users are only affected by the first case. The third, dual-frequency user case however must protect against all three fault modes (with smaller error limits). Single frequency users have only a single pseudorange signal, ρ_{L1}, that requires monitoring. To remove ionospheric errors, dual frequency users will use ρ_{DF}, that incorporates information from the ranging signal on L5, ρ_{L5}.

The dual-frequency pseudorange is modified according to the equation below.

$$\rho_{DF} = 2.26\rho_{L1} - 1.26\rho_{L5} \quad (1)$$

A simultaneous fault on both signals assumes the same threat reflection parameters apply to each signal then maximizes ρ_{DF}. In other words, for each threat, the minimum ρ_{L5} bias over all allowed L5 receiver configurations was differenced from the maximum ρ_{L1} error over all allowed L1 receiver configurations.

Maximum Allowable Range Error Limits

The maximum allowable range errors for the faults are a function of the

- Fault-tree allocation for a signal deformation fault
- Desired false-alarm probability
- Nominal noise on the monitor and differential range measurements

A detailed derivation of the time-varying formulation explaining how it integrates the time and margin information into a single pass-fail test for meeting the current WAAS fault tree allocation for these faults is provided in Appendix A of [5]. This paper analyzes only the time-variant case where the fault is assumed to be present on the satellite signal at launch, the WAAS broadcast range error limits are at a minimum (i.e., UDREIs are at their floor values), and the detection capability of the WAAS network is maximized.

RESULTS

The analysis techniques detailed in [3] and [5] were used to compute all subsequent results for receiver errors, error limits, and WAAS monitor receiver metrics.

Figures 4 and 5 plot the maximum range errors vs monitor response corresponding to the single-reflection threats of Table 1 for the relative reflection delays, $d \leq 20$ m and for monitor attenuation factors β=1 and β=0.6, respectively. In both figures, the error limits (i.e., the dashed red lines) are not exceeded crossed by the maximum user errors in the multipath threat model. Only when the monitor attenuation 40% attenuation, do a few threats exceed the error limit for single-frequency users. This is shown in Figure 5, for β=0.5.

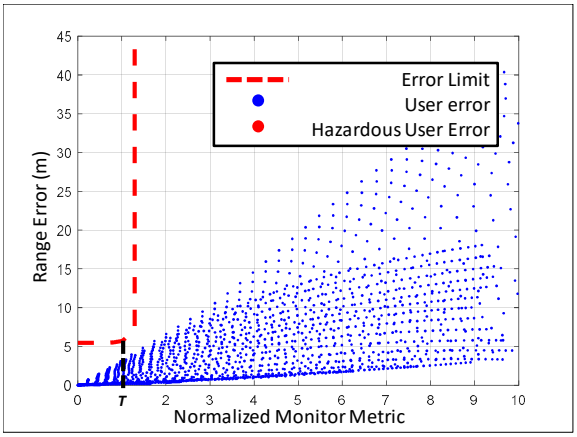

Figure 4. Error vs Monitor Response ($\beta = 1.0$) for single-frequency WAAS users at minimum error limit of 5.5 m (UDREI=5). Relative delays, $d \leq 20$ m.

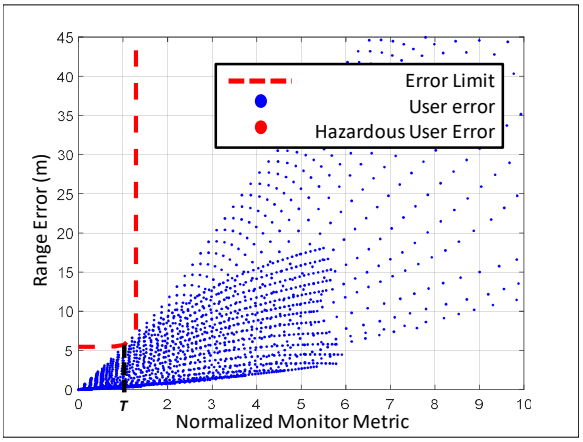

Figure 5. Error vs Monitor Response ($\beta = 0.6$) for single-frequency WAAS users at minimum error limit of 5.5 m (UDREI=5). Relative delays, $d \leq 20$ m.

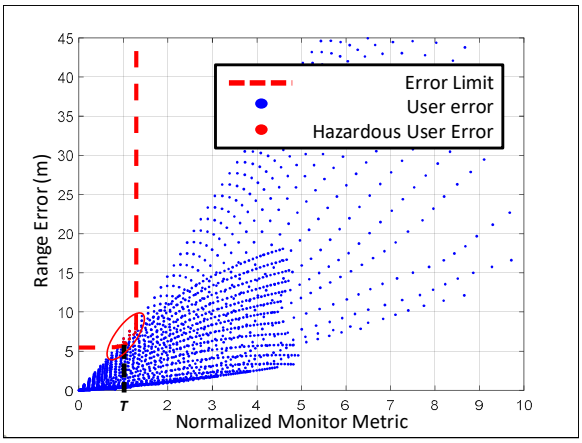

Figure 6. Error vs Monitor Response ($\beta = 0.5$) for single-frequency WAAS users at minimum error limit of 5.5 m (UDREI=5). Relative delays, $d \leq 20$ m.

Figure 7 plots the reflection parameters corresponding to the threats from Figure 6, where, for reflection relative delays below 20 meters, the range errors exceed the error limit. Note that the relative amplitudes of these threats are small.

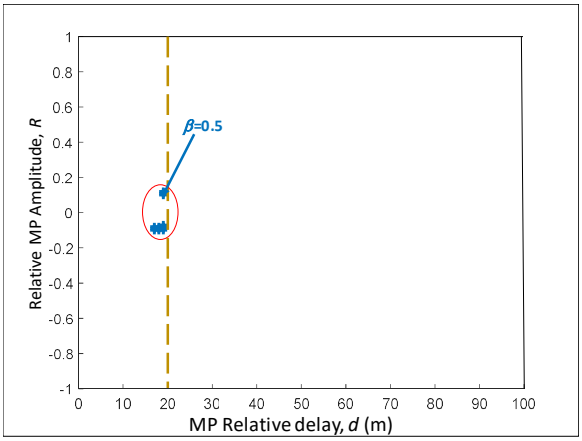

Figure 7. Hazardous, undetectable multipath parameters at monitor attenuation, β=0.5 for single-frequency WAAS users at minimum error limit of 5.5 m (UDREI=5). Relative delays, $d \leq 20$ m.

For extreme multipath threats (i.e., d >20 m), more parameters may be undetected. Figure 8 shows the hazardous, undetectable reflection parameters at 10 discrete monitor attenuation levels: $0.2 \leq \beta \leq 1.0$ Intuitively, the largest number undetectable threats correspond to the highest level of attenuation ($\beta = 0.2$) and the smallest number corresponds to the lowest ($\beta = 1.0$).

For all the hazardous multipath parameters shown in Figure 8, the user receiver configurations correspond to low-bandwidth (< 7 MHz) EML receivers. [3] This means, in addition to the monitor protecting all WAAS users against multipath with relative delays below 20 m even at 60% effectiveness, it protects all *practical* users at for delays as large as 100 m at an effectiveness of just 20% (β=0.2). Figure 9 plots the maximum user range errors vs monitor metric for this latter case.

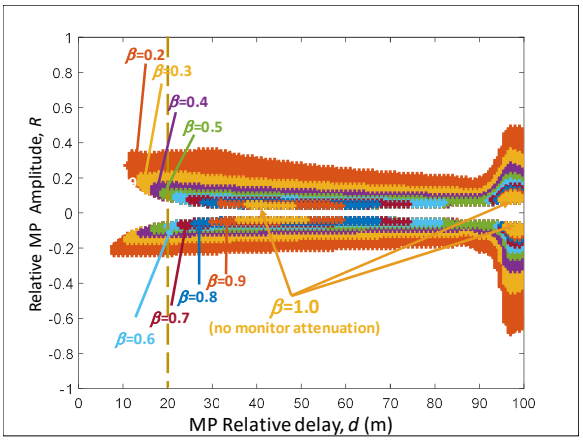

Figure 8. Hazardous, undetectable multipath parameters at various monitor attenuation levels for single-frequency WAAS users at minimum error limit of 5.5 m (UDREI=5). Relative delays, $d \leq 100$ m.

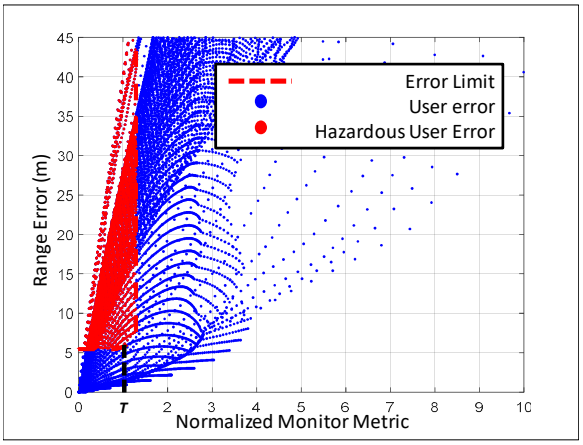

Figure 9. Error vs Monitor Response ($\beta = 0.2$) for single-frequency WAAS users at minimum error limit of 5.5 m (UDREI=5). Relative delays, $d \leq 20$ m.

For dual-frequency users—constrained to a significantly smaller receiver configuration space described in Figures 2 and 3—the theoretical minimum range error limit is extremely small (i.e., 10 mm at a UDREI = 0). The multipath threat, however, is not the only signal deformation threat. Nominal signal deformations are always present. These, too, are known create small range biases on the signals [6][7][8][9]. Analysis of these deformations on L1 and L5 yield a dual-frequency nominal range bias estimate of nearly 50 cm. (See Appendix A.) Due to quantization in the WAAS broadcast range error bounds, this sets a lower limit for the dual-frequency range error limit of approximately 0.8 meters (UDREI = 2). And it is believed that due to the presence of other range errors, even this error limit below the minimum that WAAS will ultimately be capable of supporting.

Figure 10 plots the maximum range errors vs monitor metric corresponding to dual-frequency users for the monitor attenuation case of β=0.6. It shows the monitor can protect all dual-frequency users against even extreme single-reflection SV multipath threats at an error limit of 1.5 meters (UDREI = 3) despite monitor attenuation by a factor of 10.

Note that for dual-frequency users, the L1 user range error is (still) the most significant constraint on the achievable lower limit. After differential correction, the L5 errors are relatively small. This difference is, in part, due to the ionosphere removal described by Equation 1. It's also due to the differences in signal structure of L1 C/A relative to L5. Further, as was the case for single-frequency users, substantial benefit comes from a combination of 1) inflation of the error limits due to pre-existing constraints, and 2) a reduction in the span of user receiver configurations considered.

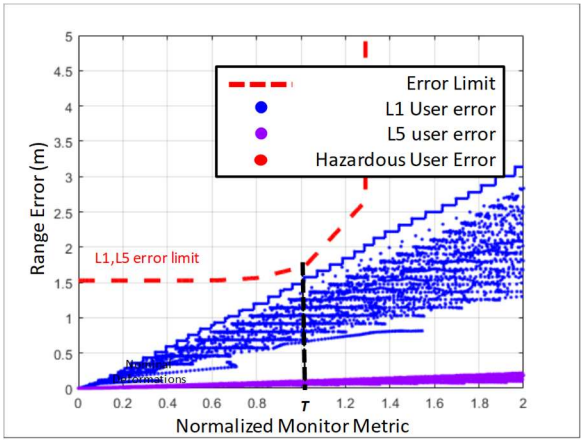

Figure 10. Error vs Monitor Response ($\beta = 0.1$) for dual-frequency WAAS users at minimum error limit of 1.5 m (UDREI = 3). Relative delays, $d \leq 100$ m.

CONCLUSION

The WAAS signal deformation monitor has been evaluated against the elevation angle-dependent multipath threat in attempt to assess its ability to protect single and dual-frequency users when the monitor has reduced effectiveness. To this end, a two-parameter single-reflection model was developed to include a wide range of possible multipath threat conditions. In addition, the elevation-angle dependent range errors (as previously observed on SVN-49) were introduced and modeled as a scalar attenuation of the WAAS monitor observations of the multipath distortion.

For standard, L1-only WAAS users, the monitor can mitigate harmful anticipated multipath threats when the monitor measurements attenuated as much as 40%. Performance improves substantially if only practical user receivers are modeled. For dual-frequency users, which substantially limits allowable receiver discriminator and bandwidth variability, the monitor can protect all users at nearly the smallest feasible error limit at an attenuation of 60%.

This analysis shows the current signal deformation threat model and the WAAS monitor protect against a variety of signal distortion threats. It also shows that additional, real-world constraints on lower range error limits and practical receiver design constraints also contribute to ensuring WAAS users are protected against them.

REFERENCES

[1] "International Standards and Recommended Practices," *Aeronautical Telecommunications*, ICAO, Vol. 1, Annex 10, July 2006.

[2] Shallberg, Karl W., Ericson, Swen D., Phelts, Eric, Walter, Todd, Kovach, Karl, Altshuler, Eric, "Catalog and Description of GPS and WAAS L1 C/A Signal Deformation Events," *Proceedings of the 2017 International Technical Meeting of The Institute of Navigation*, Monterey, California, January 2017, pp. 508-520.

[3] Phelts, R. E., Shallberg, K., Walter, T., Enge, P., "WAAS Signal Deformation Monitor Performance: Beyond the ICAO Threat Model", *Proceedings of the ION 2017 Pacific PNT Meeting*, Honolulu, Hawaii, April 2017.

[4] Minimum Operational Performance Standards (MOPS) for WAAS, DO-229D. *RTCA*.

[5] Phelts, R. E., Wong, G., Walter, T., Enge, P., "Signal Deformation Monitoring for Dual-Frequency WAAS," Proceedings of ION ITM, San Diego, CA, January 2013.

[6] Wong, Gabriel, Chen, Yu-Hsuan, Phelts, R. Eric, Walter, Todd, Enge, Per, "Mitigation of Nominal Signal Deformations on Dual-Frequency WAAS Position Errors, "*Proceedings of the 27th International Technical Meeting of The Satellite Division of the Institute of Navigation (ION GNSS+ 2014)*, Tampa, Florida, September 2014, pp. 3129-3147.

[7] Wong, G., Phelts, R. E., Walter, T., Enge, P., "Measuring Code-Phase Differences Due to Inter-Satellite Hardware Differences," *Proceedings of the 25nd International Technical Meeting of the Satellite Division of the Institute of Navigation*, ION GNSS-2012, September 2012.

[8] Thoelert, S., Enneking, C., Vergara, M., Sgammini, M., Antreich, F., Meurer, M., Brocard, D., Rodriguez, C., "GNSS Nominal Signal Distortions - Estimation, Validation and Impact on Receiver Performance," *Proceedings of the 28th International Technical Meeting of The Satellite Division of the Institute of Navigation (ION GNSS+ 2015)*, Tampa, Florida, September 2015, pp. 1902-1923.

[9] Phelts, R.E., Walter, T., Enge, P., "Characterizing Nominal Analog Signal Deformation on GNSS Signals," *Proceedings of the 22nd International Technical Meeting of The Satellite Division of the Institute of Navigation (ION GNSS 2009)*, Savannah, GA, September 2009, pp. 1343-1350

Appendix A

Nominal Signal Deformation Biases

Estimates for the maximum nominal signal deformations for single-frequency and dual-frequency users derive from Figures A-1 through A-3. A summary of the estimated biases is provided in Table A-1.

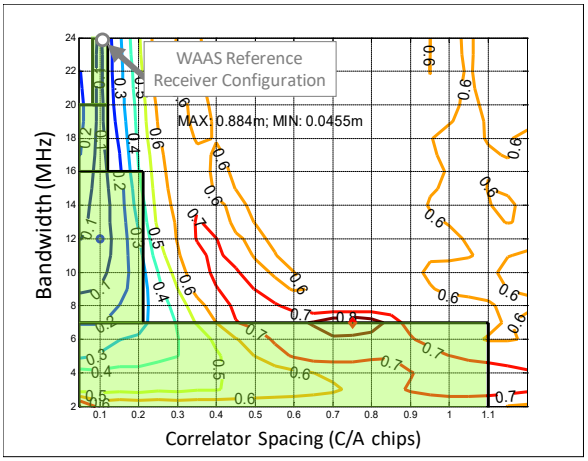

Figure A-1. Nominal signal deformation range errors on WAAS single-frequency (L1 C/A-code) users.

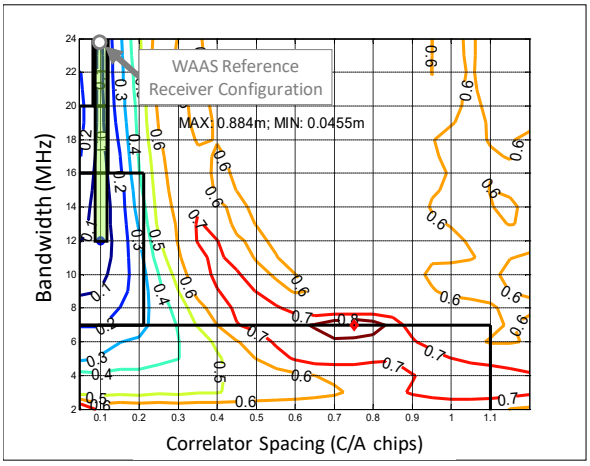

Figure A-2. Nominal signal deformation range errors on WAAS single-frequency (L1 C/A-code) users.

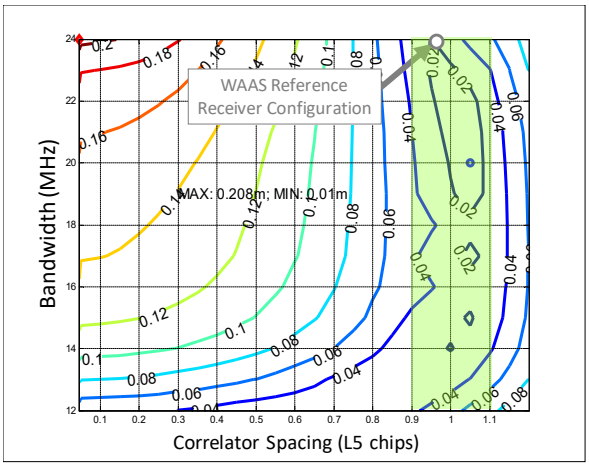

Figure A-3. Nominal signal deformation range errors on WAAS dual-frequency (L5) users.

Table A-1. Nominal Signal Deformation Biases

WAAS User Receiver	Max Range Bias (m)
Single-frequency (all)	0.9
Single-frequency (>7 MHz)	0.35
Dual-frequency	L1: 0.15 L5: 0.1 L1,L5: 0.46